Published December 1, 1986

A Time-dependent and Voltage-sensitive K^+ Current in Single Cells from Frog Atrium

MARK A. SIMMONS, TONY CREAZZO, and H. CRISS HARTZELL

From the Department of Anatomy and Cell Biology, Emory University School of Medicine, Atlanta, Georgia 30322

ABSTRACT A quantitative description of the time-dependent and voltage-sensitive outward currents in heart has been hampered by the complications inherent to the multicellular preparations previously used. We have used the whole-cell patch-clamp technique to record the delayed outward K^+ current, I_K, in single cells dissociated from frog atrium. Na^+ currents were blocked with tetrodotoxin and Ca^{2+} currents with Mn^{2+} or Cd^{2+}. After depolarizations from −50 mV to potentials positive to −30 mV, a time-dependent outward current was observed. This current has been characterized according to its steady state activation, kinetics, and ion transfer function. The current is well described as a single Hodgkin-Huxley conductance. The deactivation of the current is a single exponential. Activation of the current is sigmoid and is fitted well by raising the activation variable to the second power. The reversal potential of I_K is near E_K and shifts by 57 mV/10-fold change in $[K^+]_o$. This suggests that the current is carried selectively by K ions. The threshold for activation is near −30 mV. I_K is maximally activated positive to +20 mV and shows no inactivation. The fully activated current-voltage relationship is linear between −110 and +50 mV. Neither Ba^{2+} (250 μM) nor Cd^{2+} (100 μM) affects I_K.

INTRODUCTION

In the squid axon, depolarization elicits a fast inward Na^+ current that is followed by a slowly developing outward current carried by K ions (Hodgkin and Huxley, 1952). This current, the "delayed rectifier," is responsible for initiating repolarization of the membrane. A similar current has been described in both amphibian (Rougier et al., 1968; DeHemptinne, 1971; Maughan, 1973; Ojeda and Rougier, 1974; Brown et al., 1976*a–c*, 1980; Giles and Noble, 1976; Hume and Giles, 1983) and mammalian heart (McAllister and Noble, 1966; D. Noble and Tsien, 1969*a, b*; Katzung and Morgenstern, 1977; McDonald and Trautwein, 1978; DiFrancesco et al., 1979; Kokubun et al., 1982).

There is considerable disagreement, however, about the nature of the time-dependent outward current in heart. The number of currents present, the activation ranges and kinetics of the currents, their selectivity for K^+, and their functions in initiating or controlling repolarization have remained unclear (see

Address reprint requests to Dr. Mark A. Simmons, Dept. of Anatomy and Cell Biology, Emory University School of Medicine, Atlanta, GA 30322. Dr. Creazzo's present address is Dept. of Anatomy, Medical College of Georgia, Augusta, GA 30912.

J. GEN. PHYSIOL. © The Rockefeller University Press · 0022-1295/86/12/0739/17$1.00

Volume 88 December 1986 739–755

Downloaded from jgp.rupress.org on May 1, 2016

Published December 1, 1986

reviews by Carmeliet and Vereecke, 1979, and D. Noble, 1984). Many previous studies have used multicellular preparations, which are difficult to space-clamp adequately. The large series resistance that is usually encountered can also introduce significant errors in the measurement of membrane potential (Johnson and Lieberman, 1971; New and Trautwein, 1972; Attwell and Cohen, 1977). Furthermore, K^+ currents can result in the accumulation of K^+ in narrow extracellular spaces and a change in the equilibrium potential for K^+ (Maughan, 1973; Brown et al., 1976*b*, 1980; S. J. Noble, 1976; Attwell and Cohen, 1977; Kline and Morad, 1978; Attwell et al., 1979; Morad, 1980; Lammel, 1981; Cohen and Kline, 1982).

The whole-cell patch-clamp technique (Neher and Sakmann, 1976; Hamill et al., 1981) of single, isolated cells (Isenberg and Klockner, 1982; Hume and Giles, 1983; for references see Trube, 1983; Bkaily et al., 1984) circumvents many of the shortcomings of multicellular preparations.

Hume and Giles (1983) have examined I_K in single dissociated cells from frog atrium using a variation of the whole-cell patch-clamp technique. They provided evidence that I_K was carried mainly by K ions, that accumulation and depletion were not a major problem in this preparation, and that I_K could be explained by a single Hodgkin-Huxley–type conductance. In this article, using different conditions, we have confirmed the findings of Hume and Giles (1983) and, in addition, have characterized I_K in detail with respect to its ion transfer function, activation, kinetics, and sensitivity to Ba^{2+} and Cd^{2+}. Recently, Giles and Shibata (1985) have completed an analysis of I_K in primary pacemaker cells of the frog sinus venosus. The characteristics of I_K are very similar in primary pacemaker tissue and in the atrium. A preliminary note has appeared (Simmons and Hartzell, 1985).

METHODS

Drugs and Solutions

The compositions of Ringer solutions were (in mM): normal Ringer: 115 NaCl, 4 KCl, 2 $CaCl_2$, 1 $MgCl_2$, 10 HEPES, pH 7.4; Mn Ringer: 112 NaCl, 4 KCl, 0.1 $CaCl_2$, 4 $MnCl_2$, 10 HEPES, pH 7.4; Cd Ringer: 117 NaCl, 4 KCl, 0.1 $CaCl_2$, 10 HEPES, 0.1 $CdCl_2$, pH 7.4. The composition of the intracellular medium was (mM): 120 KCl, 0.5 $MgCl_2$, 0.3 NaH_2PO_4, 1 EGTA, 2 Na_2ATP, 0.2 Na_2GTP, 5 HEPES, pH 7.6 (adjusted with KOH). Extracellular $[K^+]$ was changed by equimolar substitution of KCl for NaCl. Tetrodotoxin (TTX) (1 μM) was routinely added to the extracellular medium to block the fast Na^+ current. All experiments were performed at 20°C. TTX, type I collagenase, type II trypsin from bovine pancreas, and bovine serum albumin were obtained from Sigma Chemical Co., St. Louis, MO.

Dissociation of Cells

Frogs, *Rana pipiens*, were used. The heart was removed and the atrium was dissected in normal Ringer solution. The dissociation was performed by a modification of the method of Hume and Giles (1983) in normal Ringer with $CaCl_2$ reduced to 8 μM in petri dishes agitated on an orbital shaker. The atrium was incubated for 75 min in 200 U/ml collagenase plus 2,000 U/ml trypsin, rinsed for 5 min in 0.1% bovine serum albumin, and then incubated for 1.5 h in 100 U/ml collagenase. The tissue was transferred to Mn

Downloaded from jgp.rupress.org on May 1, 2016

Published December 1, 1986

Ringer or Cd Ringer and gently triturated with a 5-ml pipette to dissociate single cells. After allowing the cells to attach to the dish (~15 min), the dishes were placed in the patch-clamp setup and constantly superfused with Ringer solution at a rate of ~0.75 ml/min.

Electrophysiology

The whole-cell recording configuration of the patch-clamp technique (Hamill et al., 1981) was used for voltage-clamping single dissociated cells (Hume and Giles, 1983; Fischmeister and Hartzell, 1986). Patch-clamp electrodes, pulled on a vertical puller, coated with Sylgard, and fire-polished (Corey and Stevens, 1983), had resistances of 1–5 MΩ. The electrode was filled with intracellular medium. A List EPC-7 (List Medical-Electronic, Darmstadt, Federal Republic of Germany) amplifier was used for recording cell currents. The establishment of whole-cell recording was confirmed by monitoring the increase in capacitance as the patch was broken and by monitoring resting membrane potential in the current-clamp mode after patch disruption. Total series resistance (including pipette resistance) ranged from 2 to 10 MΩ; typically, >50% of the series resistance could be compensated (Sigworth, 1983). In most experiments, the uncompensated series resistance was <2 MΩ. If the uncompensated series resistance was >10 MΩ, the cell was not used. Since the maximum current activated in a cell was ~1.5 nA, voltage errors caused by series resistance will be small at the maximum currents recorded and negligible near the reversal potential. Previous experiments have demonstrated that adequate voltage homogeneity of these cells is achieved (Fischmeister and Hartzell, 1986).

Voltage-Clamp Protocols and Terminology

Voltage steps were made by means of a programmable digital stimulator designed and constructed by Mr. William N. Goolsby (Dept. of Anatomy and Cell Biology, Emory University). Voltage steps were made from a holding potential (E_H) to various clamp potentials (E_C), followed by a step to a test potential (E_T). The currents flowing in response to these steps are named by the convention $I(E, t)$, where I is the current flowing at time t after the step to the potential E.

Exponential Curve-Fitting

For curve-fitting, data acquisition was begun between 10 and 50 ms after the voltage step. The tail currents illustrated were fitted to sums of exponentials by the Marquardt method of iterative least squares. Recently, however, these results have been verified using an algorithm developed by E. Yeramian (Institut Pasteur, Paris). The algorithm does not require any a priori hypothesis about the number of components and is based on the combined use of Laplace transforms and Pade approximants. The principle of the method is similar to that described by Isenberg and co-workers (see references in Isenberg and Small, 1982).

RESULTS

Morphology of Dissociated Frog Atrial Cells

Fig. 1*A* is a Nomarski micrograph of a single cell dissociated from a frog atrium. This cell is typical of the cells that were used for voltage-clamp experiments. The dimensions of 62 fixed cells in 10 randomly selected low-power micrographs were measured by tracing enlargements of images on a digitizing pad attached to a computer (Hartzell and Sale, 1985). Only single cells, identified by the

Downloaded from jgp.rupress.org on May 1, 2016

Published December 1, 1986

presence of a single nucleus, were measured. The mean length was 227 ± 112 μm (mean ± 95% confidence interval; range, 128–360 μm). The cells were somewhat tapered and their diameter varied along the length of the cell, as shown in the electron micrograph of Fig. 1*B*. Near the nucleus, the typical diameter was 5–6 μm, whereas at the ends of the cell, the diameter was closer to

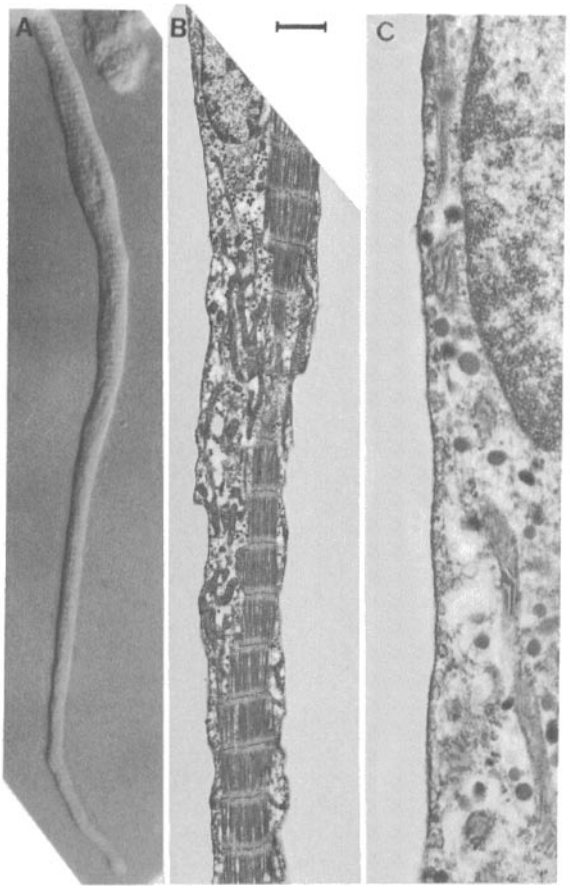

FIGURE 1. Micrographs of dissociated cells from frog atrium. Cells were dissociated as described in the Methods. (*A*) Nomarski micrograph of a living frog atrial cell. Calibration bar, 20 μm. (*B*) Electron micrograph of a different atrial cell. Calibration bar, 2 μm. (*C*) Higher magnification of a region of the cell shown in *B*. Calibration bar, 0.4 μm. The dissociated cells were fixed for 1 h by immersion in Ringer containing 1% glutaraldehyde, postfixed in 1% osmium tetroxide, dehydrated, and embedded in Embed-Araldite.

2 μm. For electrophysiological experiments, we selected relaxed cells. We did not routinely measure the length of these cells, but the average length of 14 cells used for electrophysiology was 281 ± 76 μm. Assuming a specific capacitance of 1 $\mu F/cm^2$, one would expect a cylindrical cell 280 μm long and 5 μm in diameter to have a capacitance of 44 pF. The average measured capacitance of these 14 cells was 64 ± 37 pF. The difference between the expected and the observed

Downloaded from jgp.rupress.org on May 1, 2016

Published December 1, 1986

values is probably explained by the infoldings of the plasma membrane, which can be observed in the high-power electron micrograph of Fig. 1*C*.

The sarcomere length was 2.0–2.1 μm (Fig. 1*B*), which was identical to that measured in intact frog atrium (Hartzell, H. C., and W. S. Sale, unpublished data). The dissociated cells had large clear areas and very little identifiable sarcoplasmic reticulum, but we are uncertain whether this was due to artifacts induced by fixation or was due to the dissociation procedure. Atrial specific granules were prominent in the nuclear region.

Time-dependent Outward Current

Time-dependent outward currents were examined by the protocols shown in Fig. 2. In Fig. 2*A*, 11-s depolarizations to various potentials were made from E_H

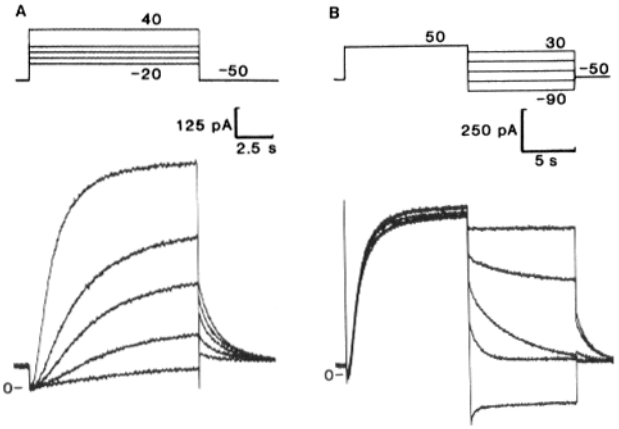

FIGURE 2. Membrane currents in single frog atrial cells. Voltage is shown on the top and current is shown on the bottom. (*A*) Protocol used to study the activation of I_K. The current was activated by voltage steps from $E_H = -50$ mV to various E_C values (+40, +10, 0, −10, and −20 mV are shown), followed by a return to $E_T = -50$ mV. (*B*) Protocol used to determine ion transfer function and τ_n for deactivation of I_K. I_K was fully activated by depolarization from $E_H = -50$ mV to $E_C = +50$ mV. The cell was then repolarized to various E_T values (+30, 0, −30, −60, and −90 mV are shown).

= −50 mV. After an instantaneous decrease in current caused by the negative slope conductance of I_{K1} in this range of potentials (Simmons and Hartzell, 1985), an outward current slowly developed. The delayed outward current reached a steady state level with a time constant of several seconds and showed no signs of inactivation, even with clamp pulses as long as 20 s.

Reversal Potential

To determine the K^+ selectivity of this current, the reversal potential (E_{rev}) was measured in 2, 4, 10, and 20 mM $[K^+]_o$ (Fig. 3*A*). The membrane was depolarized from −50 to +50 mV for 10 s to activate I_K fully. The membrane was then stepped to various test potentials and the voltage at which the current tails reversed was measured. The reversal potential of the current tails was typically

Downloaded from jgp.rupress.org on May 1, 2016

Published December 1, 1986

5 mV positive to the calculated E_K. In Fig. 3*B* (squares), the reversal potential was plotted as a function of $[K^+]_o$. The slope of the resulting line was 57 mV/10-fold change in $[K^+]_o$, which was very close to the expected value of 59 mV if I_K were specifically permeable to K^+.

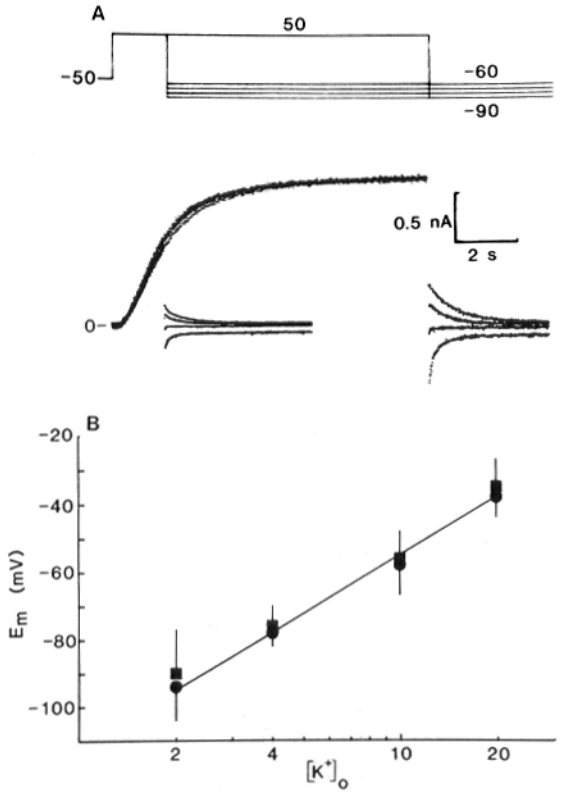

FIGURE 3. Effects of extracellular K^+ on the reversal potential of I_K. (*A*) Sample of current tracings used to determine E_{rev}. Voltage is shown on the top and current is shown on the bottom. This record was obtained in 4 mM $[K^+]_o$. The membrane was stepped from $E_H = -50$ mV to $E_C = +50$ mV for 2 or 10 s and then clamped to $E_T = -60$, -70, -80, or -90 mV. Note that the current tails reverse near -80 mV after either a 2- or 10-s pulse. The clamp potentials were shifted accordingly for the determination of E_{rev} in different $[K^+]_o$. (*B*) Dependence of E_{rev} on $[K^+]_o$. (Circles) Mean E_{rev} after a 2-s pulse. (Squares) Mean E_{rev} after a 10-s pulse. $n = 5$ cells. Bars indicate 95% confidence intervals for each point. The line is the least-squares fit to the data and exhibits a slope of 57 mV/10-fold change in $[K^+]_o$.

K^+ Accumulation

One would not expect K^+ accumulation to occur to the same extent in single, isolated cells as in multicellular preparations, where the extracellular space is much smaller. However, the electron micrograph of Fig. 1*C* demonstrates that there are numerous small caveolae of the plasma membrane in these cells. These

Downloaded from jgp.rupress.org on May 1, 2016

Published December 1, 1986

caveolae present a possible site of K^+ accumulation. To determine whether accumulation or depletion of K^+ was occurring during the long voltage steps that we used to characterize this current, E_{rev} was compared after activation of the current for 2 or 10 s. If accumulation of K^+ around the cell occurred during the pulse, one would expect the reversal potential to be shifted in a positive direction with progressively longer depolarizing pulses. The membrane was stepped to −60, −70, −80, or −90 mV after a 2- or 10-s step from −50 to +50 mV (Fig. 3*A*). The E_{rev} obtained at 2 s (Fig. 3*B*, circles) was not statistically different from the E_{rev} obtained at 10 s (Fig. 3*B*, squares).

Basis for the Characterization of I_K

We have found that I_K is well described by a classical Hodgkin-Huxley scheme of the form: $I_K = n^p\bar{I}_K$, where n is the activation variable raised to the power p and $\bar{I}_K$ is the fully activated current (Hodgkin and Huxley, 1952). With this model, I_K can be fully described according to its kinetics, activation range, and conductance with the protocols shown in Fig. 2.

Sigmoid Onset of I_K

The sigmoid time course of the activation of I_K (Fig. 2*A*) indicated that $p > 1$. To determine the value of p, activating currents elicited by steps from $E_H = -80$ to −40 mV to E_C from −20 to +50 mV (as shown in Fig. 2*A*) were fitted to:

$$I(t) = I(E_C, 10)\cdot[1 - \exp(-t/\tau_n)]^p.$$

Fig. 4*A* shows the nonlinear least-squares fit to the activating current after a voltage step from −50 to +20 mV. For the dashed line, $p = 1$; for the solid line, $p = 2$; for the dotted line, $p = 3$. The best fit for the activating current was obtained with a single exponential with $p = 2$.

Decay of Tail Currents

We have fitted deactivating currents (tail currents) elicited by steps from E_C = +50 mV to E_T from +30 to −110 mV to sums of exponentials of the form:

$$I(t) = I(E_T, 0)\cdot\exp(-t/\tau).$$

When E_T was positive to −30 mV, the current tail was composed of two exponential components. When E_T was hyperpolarized to −30 mV or more, the majority of the tails were fitted best by a single exponential. This finding could be explained either by assuming the presence of two conductances or by assuming that $p > 1$. According to the Hodgkin-Huxley model, after a step change in voltage, n changes with time according to:

$$n(t) = n_\infty + (n_0 - n_\infty)\exp(-t/\tau_n),$$

where n_0 = the initial value of n and n_∞ = the final value of n. Since the fits of the onset of the current indicated that I_K is best described by n^2, and since at +50 mV the current is fully activated, i.e., $n_0 = 1$,

$$n^2(t) = n_\infty^2 + 2n_\infty(1 - n_\infty)\exp(-t/\tau_n) + (1 - n_\infty)^2\exp(-2t/\tau_n)^2.$$

Downloaded from jgp.rupress.org on May 1, 2016

Published December 1, 1986

Thus, a current tail composed of two exponentials would be expected, unless $n_\infty = 0$, when the equation simplifies to $n^2(t) = \exp(-2t/\tau_n)$. Thus, when $n_0 = 1$ and $n_\infty = 0$, the current tail will be composed of a single-exponential component. Consequently, we have fitted deactivating tails elicited by steps from $E_C = +50$ mV to $E_T = -30$ to -110 mV to $I(t) = I(E_T, 0) \exp(-2t/\tau_n)$. Fig. 4*B* shows the

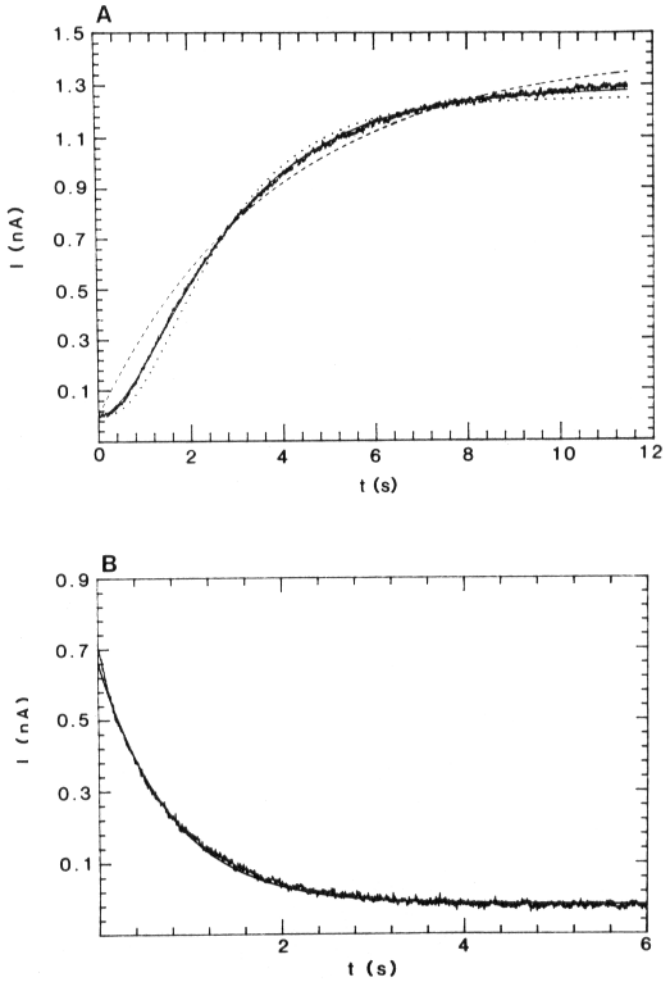

FIGURE 4. Mathematical fits of activating and deactivating I_K currents. (*A*) Activating current in response to a voltage step from $E_H = -50$ mV to $E_C = +20$ mV. The current was fitted to an equation of the form $I(t) = I(E_C, 11)\,[1 - \exp(-t/\tau)]^p$ for $p = 1$, $p = 2$, and $p = 3$. For the dashed line, $I(t) = 1.25\,[1 - \exp(-t/1.54)]^1$; for the solid line, $I(t) = 1.29\,[1 - \exp(-t/1.99)]^2$; for the dotted line, $I(t) = 1.42\,[1 - \exp(-t/3.82)]^3$. (*B*) Deactivating current in response to a hyperpolarizing pulse from $E_C = +50$ mV to $E_T = -50$ mV. The line is fitted to the single exponential $I(t) = 0.68\,[\exp(-t/1.6)]^2 - 0.02$.

Downloaded from jgp.rupress.org on May 1, 2016

Published December 1, 1986

deactivating current for return to −50 from +50 mV. The single-exponential nature of the decay of the current tails is also shown in Fig. 5*C*, where deactivating current tails are plotted on semilogarithmic coordinates.

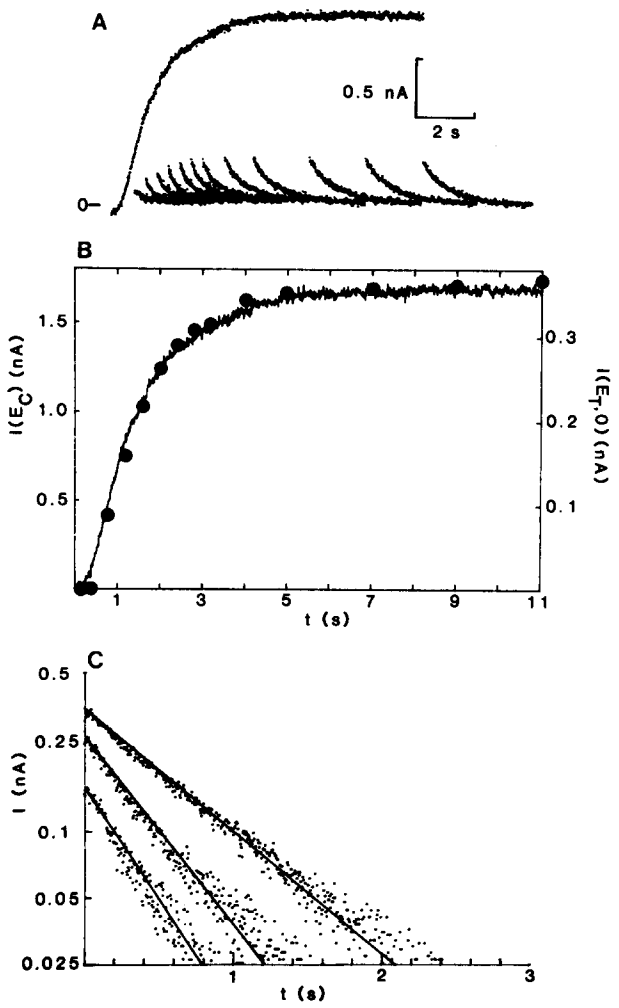

FIGURE 5. Envelope-of-tails test for I_K. (*A*) Activating current after an 11-s step from E_H = −60 mV to E_C = +50 mV with superimposed tails after the return to E_T = −60 mV at 0.8, 1.2, 1.6, 2, 2.4, 2.8, 3.2, 4, 5, 7, 9, or 11 s. No tails were observed after 0.1-, 0.2-, or 0.4-s steps. (*B*) Comparison of tail amplitudes with activating current. The left axis is the scale for the activating current trace, $I(E_C)$. The right axis is scaled for the tail amplitudes, $I(E_T, 0)$, obtained from *A* and plotted as circles. (*C*) Tails after 1.2-, 2-, and 4-s steps plotted on log scale. Points were digitized every 5 ms. The lines are single-exponential fits to the data. For the tail after the 1.2-s step, $I(t) = 0.16 \exp(-t/0.39)$; after the 2-s step, $I(t) = 0.26 \exp(-t/0.51)$; after the 3-s step, $I(t) = 0.34 \exp(-t/0.79)$.

Downloaded from jgp.rupress.org on May 1, 2016

Published December 1, 1986

Envelope of Tails

Two assumptions involved in our analysis of this current are that (*a*) the amplitude of the current tails is a quantitative measure of the size and time course of the current and (*b*) the current does not have a time-dependent component (Hodgkin and Huxley, 1952; Giles and Shibata, 1985). To test these assumptions, the time course of the "envelope of tails" was compared with the time course of I_K. I_K was activated by a voltage step from $E_H = -60$ mV to $E_C = +50$ mV, followed by a step to $E_T = -60$ mV after 0.1, 0.2, 0.4, 0.8, 1.2, 1.6, 2, 2.4, 2.8, 3.2, 4, 5, 7, 9, or 11 s. Fig. 5*A* shows the activating current and the current tails after the last 12 steps. After depolarizations for 0.1, 0.2, or 0.4 s, no current tails were measurable. In Fig. 5*B*, the onset of the current, $I(E_C)$, is plotted and compared with the peak of the current tails, $I(E_T, 0)$. Note that the envelope in Fig. 5*B*

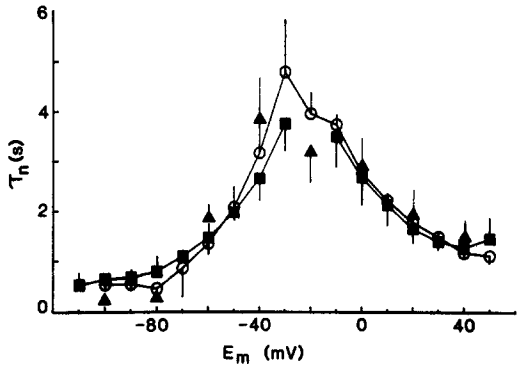

FIGURE 6. Time constant of the activation variable n. Time constants of activation were obtained by fitting activating currents after depolarizing voltage steps from $E_H = -50$ mV to $E_C = -20$ to +50 mV to the equation $I(t) = I(E_C, 11)[1 - \exp(-t/\tau_n)]^2$. Time constants of deactivation were obtained by fitting deactivating tails after hyperpolarizing steps from $E_C = +50$ mV to $E_T = -30$ to -110 mV to the equation $I(t) = I(E_T, 0)[\exp(-t/\tau_n)]^2$. (Circles) Control. (Squares) 250 μM Ba^{2+}. (Triangles) 100 μM Cd^{2+}. Bars indicate 95% confidence intervals. $n = 5$ cells.

also exhibits a sigmoidal shape and that the tail amplitudes accurately reflect the activation of I_K.

The decaying tails after 1.2-, 2-, and 4-s steps are plotted on a log scale in Fig. 5*C*. Note that the current decays as a single exponential independently of the amount of activating current. This further supports the assumption that the current being studied consists of a single component.

Kinetics

The time constants calculated from the mathematical fits of the activating and deactivating currents are plotted in Fig. 6. The time constant of the current was slowest, with a value of ~5 s near −30 mV, and declined to a minimum value of <1 s at very positive and negative membrane potentials. The time constants of activation and deactivation of I_K in Mn Ringer (circles), Cd Ringer (triangles), and in Mn Ringer containing 250 μM Ba^{2+} (squares) were statistically indistinguishable.

Downloaded from jgp.rupress.org on May 1, 2016

Published December 1, 1986

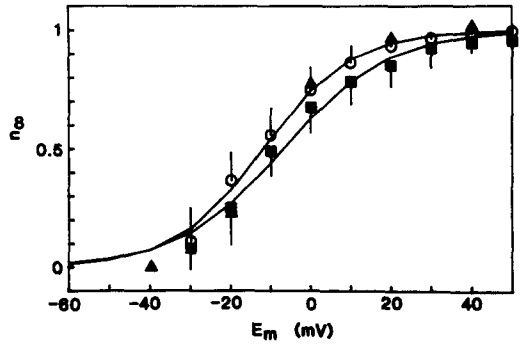

FIGURE 7. Steady state activation curve for I_K. The degree of activation, n_∞^2, was determined from the protocol of Fig. 2*A* and normalized to the maximum current for each cell, I_{max} (E_T, 0). (Circles) Mn Ringer. (Squares) 250 μM Ba^{2+}. (Triangles) Cd Ringer. The lines show the least-squares fits for the data obtained in Mn Ringer, $n_\infty = 1/\{1 + \exp[(-14 - E_m)/12]\}$, and for the data obtained in Mn Ringer plus 250 μM Ba^{2+}, $n_\infty = 1/\{1 + \exp[(-7 - E_m)/13]\}$. Bars indicate 95% confidence intervals for each point. $n = 5$ cells.

Steady State Activation

The protocol shown in Fig. 2*A* was used to examine the steady state activation. Depolarizations were made to different E_C values from $E_H = -50$ mV. The current was allowed to plateau and the membrane was then repolarized to a constant E_T of -50 mV. The amplitudes of the decaying tail currents, $I(E_T, 0)$, upon repolarization were measured and plotted against E_C. The activation curves were normalized with respect to the calculated maximum tail current, $I_{max}(E_T, 0)$, for that cell to obtain values of n_∞^2. Fig. 7 illustrates the mean normalized values of n_∞ for cells in Mn Ringer (circles), Mn Ringer containing 250 μM Ba^{2+} (squares), and Cd Ringer (triangles). This current did not activate at potentials negative to -50 mV and was almost fully activated at +20 mV. Neither Ba^{2+} nor Cd^{2+} had an effect on the activation of I_K.

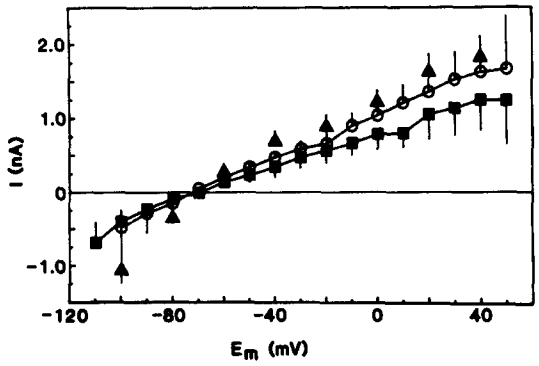

FIGURE 8. Fully activated current-voltage relation for I_K obtained by a combination of methods as described in the text. (Circles) Control. (Squares) 250 μM Ba^{2+}. (Triangles) 100 μM Cd^{2+}. Bars indicate 95% confidence intervals. $n = 5$ cells.

Downloaded from jgp.rupress.org on May 1, 2016

Published December 1, 1986

Voltage Dependence

The fully activated current-voltage relationship for I_K is shown in Fig. 8. Each point represents the average of five cells. Three types of measurement were used to determine the ion transfer function. (*a*) We used the rectifier-ratio method (Noble and Tsien, 1968). Cells were depolarized from $E_H = -50$ mV to different E_C values between −10 and +50 mV for 11 s, followed by repolarization to $E_T = -50$ mV, as shown in Fig. 2*A*. $I(E)$ was calculated from the equation

$$I(E) = \{[I(E_C, 10) - I(E_C, 0)]/[I(E_T, 0) - I(E_T, 10)]\}I_{max}(E_T, 0),$$

and plotted vs. E_C. (*b*) $I(E)$ was calculated from the tail currents elicited by repolarizing the membrane to different E_T values from −110 to +10 mV after first fully activating I_K with a conditioning pulse to +50 mV, as shown in Fig. 2*B*. $I(E)$ was calculated from the equation

$$I(E) = [I(E_T, 0) - I(E_T, 10)]/dn_\infty^2,$$

where dn_∞^2 is the difference in activation, n_∞^2, between E_C and E_T. $I(E)$ was then plotted vs. E_T. (*c*) $I(E)$ was measured directly from the initial amplitudes of the tail currents $[I(E_T, 0)]$ elicited by hyperpolarizing steps from +50 mV to different E_T values between 0 and −80 mV, as shown in Fig. 2*B*. In the voltage ranges where these three methods overlapped, the different methods gave the same results. The ion transfer function was linear from −110 to +50 mV. There was no significant effect of Ba^{2+} or Cd^{2+} on the fully activated *I-V* relationship (Fig. 8).

DISCUSSION

In these studies, we have characterized the time- and voltage-dependent outward current, I_K, in single cells from frog atrium. Our data show that this current is carried selectively by K ions, behaves as an ohmic conductance in the range of −110 to +50 mV, and can be described by a single Hodgkin-Huxley conductance with a squared activation variable. These studies confirm and extend the original observations on I_K in isolated frog atrial cells by Hume and Giles (1983). Our results and those of Hume and Giles (1983) differ significantly from some previous studies of I_K, both in amphibian and mammalian tissues.

Number of Components

Brown and collaborators (1976*a–c*, 1977, 1980) have suggested that the delayed outward current is best explained by two membrane conductances, one slow, $I_{x,slow}$, and one fast, $I_{x,fast}$. In addition, Brown et al. (1980) describe a third component that results from K^+ accumulation in the extracellular clefts. Ojeda and Rougier (1974) also observed a fast and a slow component, although some preparations exhibited only a single component. DeHemptinne (1971), on the other hand, described only a single component of delayed rectification.

Our data suggest that I_K is composed of only a single conductance because, when the power of the activation variable is taken into account, the activation and inactivation kinetics of I_K are consistently described by single-exponential functions. This description of I_K as a single current is in agreement with studies

Downloaded from jgp.rupress.org on May 1, 2016

Published December 1, 1986

on I_K in single cells from frog sinus venosus (Giles and Shibata, 1985) and atrium (Hume and Giles, 1983). The differences between these recent studies and previous ones are most easily explained by the differences between single cells and multicellular preparations. The technical problems associated with voltage-clamping multicellular preparations are well documented (Johnson and Lieberman, 1971; New and Trautwein, 1972; Attwell and Cohen, 1977). In addition, it is known that extracellular K^+ accumulation occurs during the long voltage-clamp pulses used to study I_K (Maughan, 1973; Brown et al., 1976*c*, 1977, 1980; S. J. Noble, 1976; Attwell and Cohen, 1977; Kline and Morad, 1978; Attwell et al., 1979; Morad, 1980; Lammel, 1981; Cohen and Kline, 1982). One of the currents identified in the sucrose-gap voltage-clamp studies closely resembles the I_K described here. The other currents in the sucrose gap experiments are probably related to K^+ accumulation, even though theoretical arguments (Brown et al., 1980) have suggested that these currents were not due to K^+ accumulation.

K^+ accumulation does not seem to occur to any significant extent in these isolated cells, as first shown by Hume and Giles (1983). The reversal potential of I_K does not shift after long depolarizing pulses, and the resting membrane potential is the same immediately before and after a long voltage-clamp pulse (Hartzell, H. C., unpublished data).

In other cardiac cell types, however, I_K may actually be composed of two conductances. Studies in mammalian heart tissues have commonly identified two conductances (see Carmeliet and Vereecke, 1979, for review). For example, in Purkinje fibers (Noble and Tsien, 1969*a*), in small aggregates of chicken atrial cells (Shrier, A., and J. R. Clay, personal communication), and in single cells isolated from rabbit nodal tissue (Irisawa, 1984), I_K appears to be composed of two conductances. Recently, however, Gintant et al. (1985) have suggested that I_K in Purkinje fibers decays as a sum of two exponentials because I_K is composed of one conductance with at least two closed states.

Kinetics of I_K

We consistently observed that I_K exhibited a sigmoid onset. This sigmoid onset was present regardless of the holding potential before the pulse, which suggests that the sigmoid onset was not due to other contaminating time- or voltage-dependent inward currents. The sigmoid onset of I_K might suggest that this current was a Ca^{2+}-activated K^+ conductance. However, this current is not affected by Ca^{2+} antagonists such as Cd^{2+} or Mn^{2+}. Furthermore, the current was present even though the cells were perfused with 1 mM EGTA.

Comparison of I_K in Atrial and Primary Pacemaker Cells

Recently, Giles and Shibata (1985) have published an analysis of I_K in primry pacemaker cells of the frog sinus venosus. There are several important differences between our results and techniques and those of Giles and Shibata (1985). In our experiments, the slow inward Ca^{2+} current was inhibited with Mn^{2+} or Cd^{2+} and our intracellular medium contained a solution with 125 mM K^+, compared with 1 M K^+ in the experiments of Giles and Shibata (1985). Table I compares several features of I_K in the two cell types. The most notable difference

Downloaded from jgp.rupress.org on May 1, 2016

Published December 1, 1986

is in the activation curve. In the atrial cells, the threshold for activation of I_K appears to be ~15 mV positive to the threshold in sinus cells. In addition, the fully activated *I-V* in the sinus cells inwardly rectifies above −30 mV, whereas in atrial cells the *I-V* curve is linear at least to +40 mV. It is not clear whether these differences are related to technique or whether they have physiological importance. However, it is notable that the threshold for activation of I_{Ca} in atrial cells is also 10–15 mV positive (Fischmeister, R., and H. C. Hartzell, unpublished data) to that reported for sinus cells (Shibata and Giles, 1985).

Function of I_K

The activation range and the kinetics of I_K have suggested that this current is responsible for initiating repolarization during phase 2 of repolarization (see Carmeliet, 1977). By clarifying the kinetics and activation of this current in frog atrial cells, our data provide further support for this role (Figs. 6–8). These data show that I_K is activated only at potentials positive to −30 mV. Above +20 mV, I_K is completely activated, with a time constant of ~1–1.5 s. At room temperature, the frog heart beats at a frequency between 0.5 and 1/s and the action potential remains positive to +20 mV for ~400 ms. Thus, during an action potential, ~5–10% of I_K will be activated. Since the maximum I_K is 1–3 nA, 50–300 pA of current will be activated during an action potential. With a cell of 60 pF capacitance, 100 pA of current is capable of repolarizing the membrane at a rate of ~2 V/s, which is sufficient to account for the initiation of repolarization. As the membrane repolarizes, I_K will deactivate, with a time constant of decay decreasing from 1.5 s at −40 mV to 400 ms at −80 mV. Thus, a considerable amount of I_K (several tens of picoamperes) will remain activated at the time the maximum diastolic potential is reached. As I_K decays during the interbeat interval, it could play a significant role in regulating the frequency of beating and the duration of the refractory period (Carmeliet, 1977).

Recently, Giles and Shibata (1985) and Shibata and Giles (1985) have shown that I_K plays a similar role in repolarization in the pacemaker cell. In addition,

TABLE I

Comparison of I_K in Frog Sinus Venosus and Atrium

	Atrium*	Sinus venosus‡
E_{rev} in 2.5 mM $[K^+]$	−90 mV	−95 mV
Slope E_{rev} vs. $[K^+]_o$	57 mV/decade	51 mV/decade
Activation threshold	−30 mV	−45 mV
50% activation	−12 mV	−20 mV
Power of activation variable	2	2
Reactification	None	Inward
Time constant at −30 mV	4.5 s	4.0 s
Time constant at +50 mV	1.1 s	1.0 s
Time constant at −100 mV	0.4 s	0.3 s
Slope conductance§	205 S/F	155 S/F

* Data from this article.

‡ Data from Shibata and Giles (1985).

§ Slope conductance of the linear portion of the fully activated *I-V* curve divided by average cell capacitance (82 pF for sinus cells, 64 pF for atrial cells).

Downloaded from jgp.rupress.org on May 1, 2016

Published December 1, 1986

because of the slow kinetics of deactivation of I_K, the deactivation of I_K plays an important role in determining the slope of the pacemaker depolarization. The working atrial cell, in contrast to the pacemaker cell, does not normally beat spontaneously. This is partly because the atrial cell has a large background K^+ conductance (I_{K1}) (Shibata and Giles, 1985; Simmons and Hartzell, 1985), which is usually >200 S/F at potentials below −60 mV. I_{K1} keeps the membrane hyperpolarized and prevents spontaneous firing. Indeed, Giles and Shibata (1985) have shown that atrial cells will pace spontaneously if the background I_{K1} current is blocked with Ba^{2+}. We have shown here that Ba^{2+} does not significantly affect the kinetics, the activation, or the conductance of I_K. Thus, the results of Giles and Shibata (1985) strongly support the idea that I_K plays a role in determining the rate of the pacemaker depolarization in pacemaker cells.

Sensitivity to Ba^{2+}

We have previously found that Ba^{2+} blocks the background, inwardly rectifying K^+ current, I_{K1}, at a lower concentration than it blocks the acetylcholine-activated K^+ current, $I_{K(ACh)}$ (Simmons and Hartzell, 1985, and unpublished data). Both $I_{K(ACh)}$ and I_{K1}, however, are completely blocked by 250 μM Ba^{2+}. To examine further the specificity of Ba^{2+} effects on K^+ currents, we tested 250 μM Ba^{2+} on I_K. At this concentration, Ba^{2+} had no significant effect on the activation, time constants, or current-voltage relation of I_K. Consequently, it is possible for one to study the delayed K^+ current separately without interference from I_{K1} or $I_{K(ACh)}$. Ba^{2+} at higher concentrations (>1 mM) does block the time-dependent K^+ conductances in the rabbit sinoatrial node (Osterrieder et al., 1982).

We thank Mr. William N. Goolsby for excellent electronic and programming assistance. We also thank Dr. Wayne Giles for supplying unpublished data on I_K. We thank the reviewers for suggesting that we do the envelope-of-tails test.

Supported by National Institutes of Health HL-27385 to H.C.H. and National Research Service Awards NS-07117 to T.C. and NS-07315 to M.A.S.

Original version received 13 June 1985 and accepted version received 5 May 1986.

REFERENCES

Attwell, D., and I. Cohen. 1977. The voltage clamp of multicellular preparations. *Progress in Biophysics and Molecular Biology.* 31:201–245.

Attwell, D., D. Eisner, and I. Cohen. 1979. Voltage clamp and tracer flux data: effects of restricted extracellular space. *Quarterly Review of Biophysics.* 12:213–263.

Bkaily, G., N. Sperelakis, and J. Doane. 1984. A new method for preparation of isolated single adult myocytes. *American Journal of Physiology.* 247:H1018–H1026.

Brown, H. F., A. Clark, and S. J. Noble. 1976*a*. Identification of the pacemaker current in frog atrium. *Journal of Physiology.* 258:521–545.

Brown, H. F., A. Clark, and S. J. Noble. 1976*b*. Analysis of pacemaker and repolarization currents in frog atrial muscle. *Journal of Physiology.* 258:547–577.

Brown, H. F., D. Noble, and S. J. Noble. 1976*c*. The influence of nonuniformity on the analysis of potassium currents in heart muscle. *Journal of Physiology.* 258:615–629.

Brown, H. F., D. DiFrancesco, D. Noble, and S. J. Noble. 1980. The contribution of potassium accumulation to outward currents in frog atrium. *Journal of Physiology.* 306:127–149.

Downloaded from jgp.rupress.org on May 1, 2016

Published December 1, 1986

Brown, H. F., W. Giles, and S. J. Noble. 1977. Membrane currents underlying activity in frog sinus venosus. *Journal of Physiology.* 271:783–816.

Carmeliet, E. 1977. Repolarization and frequency in cardiac cells. *Journal de Physiologie.* 73:903–923.

Carmeliet, E., and J. Vereecke. 1979. Electrogenesis of the action potential and automaticity. *In* Handbook of Physiology. Vol. 1: The Heart; Section 2: The Cardiovascular System. R. M. Berne, N. Sperelakis, and S. R. Geiger, editors. Waverly Press, Inc., Baltimore, MD. 269–334.

Cohen, I., and R. Kline. 1982. K fluctuations in the extracellular spaces of cardiac muscle. Evidence from the voltage clamp and extracellular K-selective microelectrodes. *Circulation Research.* 50:1–16.

Corey, D. P., and C. F. Stevens. 1983. Science and technology of patch-recording electrodes. *In* Single Channel Recording. B. Sakmann and E. Neher, editors. Plenum Press, New York. 53–68.

DeHemptinne, A. 1971. Properties of the outward currents in frog atrial muscle. *Pflügers Archiv.* 329:321–331.

DiFrancesco, D., A. Noma, and W. Trautwein. 1979. Kinetics and magnitude of the time-dependent K current in the rabbit s. a. node: effect of external potassium. *Pflügers Archiv.* 381:271–279.

Fischmeister, R., and H. C. Hartzell. 1986. Mechanism of action of acetylcholine on calcium current in single cells from frog ventricle. *Journal of Physiology.* 376:183–202.

Giles, W., and S. J. Noble. 1976. Changes in membrane currents in bullfrog atrium produced by acetylcholine. *Journal of Physiology.* 261:103–123.

Giles, W. R., and E. F. Shibata. 1985. Voltage clamp of bull-frog cardiac pacemaker cells: a quantitative analysis of potassium currents. *Journal of Physiology.* 368:265–292.

Gintant, G. A., N. B. Datyner, and I. B. Cohen. 1985. Gating of delayed rectification in acutely isolated canine cardiac Purkinje myocytes. *Biophysical Journal.* 48:1059–1064.

Hamill, O. P., A. Marty, E. Neher, B. Sakmann, and F. J. Sigworth. 1981. Improved patch-clamp techniques for high-resolution current recording from cells and cell-free membrane patches. *Pflügers Archiv.* 391:85–100.

Hartzell, H. C., and W. S. Sale. 1985. Structure of C-protein purified from cardiac muscle. *Journal of Cell Biology.* 100:208–215.

Hodgkin, A. L., and A. F. Huxley. 1952. A quantitative description of membrane current and its application to conduction and excitation in nerve. *Journal of Physiology.* 117:500–544.

Hume, J. R., and W. Giles. 1983. Ionic currents in single isolated bullfrog atrial cells. *Journal of General Physiology.* 81:153–194.

Irisawa, H. 1984. Electrophysiology of single cardiac cells. *Japanese Journal of Physiology.* 34:375–388.

Isenberg, G., and U. Klockner. 1982. Calcium tolerant ventricular myocytes prepared by preincubation in 'KB medium.' *Pflügers Archiv.* 395:6–18.

Isenberg, I., and E. W. Small. 1982. Exponential depression as a test of estimated decay parameters. *Journal of Chemical Physics.* 77: 2799–2805.

Johnson, E. A., and M. Lieberman. 1971. Heart: excitation and contraction. *Annual Reviews of Physiology.* 33:479–532.

Katzung, B. G., and J. A. Morgenstern. 1977. Effects of extracellular potassium on ventricular automaticity and evidence for a pacemaker current in ventricular myocardium. *Circulation Research.* 40:105–111.

Downloaded from jgp.rupress.org on May 1, 2016

Published December 1, 1986

Kline, R. P., and M. Morad. 1978. Potassium efflux in heart muscle during activity: extracellular accumulation and its implications. *Journal of Physiology.* 280:537–558.

Kokubun, S., M. Nishimura, A. Noma, and H. Irisawa. 1982. Membrane currents in the rabbit atrioventricular node. *Pflügers Archiv.* 393:15–22.

Lammel, E. 1981. A theoretical study on the sucrose gap technique as applied to multicellular muscle preparations. II. Methodical errors in the determination of outward currents. *Biophysical Journal.* 36:555–573.

Maughan, D. 1973. Some effects of prolonged polarization on membrane currents in bullfrog atrial muscle. *Journal of Membrane Biology.* 11:331–352.

McAllister, R. E., and D. Noble. 1966. The time and voltage dependence of the slow outward current in cardiac Purkinje fibres. *Journal of Physiology.* 186:632–662.

McDonald, T. F., and W. Trautwein. 1978. The potassium current underlying delayed rectification in cat ventricular muscle. *Journal of Physiology.* 274:217–246.

Morad, M. 1980. Physiological implications of K accumulation in heart muscle. *Federation Proceedings.* 393:1533–1539.

Neher, E., and B. Sakmann. 1976. Single-channel currents recorded from membrane of denervated frog muscle fibres. *Nature.* 260:799–802.

New, W., and W. Trautwein. 1972. The ionic nature of slow inward current and its relation to contraction. *Pflügers Archiv.* 334:24–38.

Noble, D. 1984. The surprising heart: a review of recent progress in cardiac electrophysiology. *Journal of Physiology.* 353:1–50.

Noble, D., and R. W. Tsien. 1968. The kinetics and rectifier properties of the slow potassium current in cardiac Purkinje fibres. *Journal of Physiology.* 195:185–214.

Noble, D., and R. W. Tsien. 1969*a*. Outward membrane currents activated in the plateau range of potentials in cardiac Purkinje fibres. *Journal of Physiology.* 200:205–231.

Noble, D., and R. W. Tsien. 1969*b*. Reconstruction of the repolarization process in cardiac Purkinje fibres based on voltage clamp measurements of the membrane current. *Journal of Physiology.* 200:233–254.

Noble, S. J. 1976. Potassium accumulation and depletion in frog atrial muscle. *Journal of Physiology.* 258:579–613.

Ojeda, C., and O. Rougier. 1974. Kinetic analysis of the delayed outward currents in frog atrium. Existence of two types of preparation. *Journal of Physiology.* 239:51–73.

Osterrieder, W., Q.-F. Yang, and W. Trautwein. 1982. Effects of barium on the membrane currents in the rabbit S-A node. *Pflügers Archiv.* 394:78–84.

Rougier, O., G. Vassort, and R. Stampfli. 1968. Voltage clamp experiments on frog atrial heart muscle fibers with the sucrose gap technique. *Pflügers Archiv.* 301:91–108.

Shibata, E. F., and W. Giles. 1985. Ionic currents that generate the spontaneous diastolic depolarization in individual cardiac pacemaker cells. *Proceedings of the National Academy of Sciences.* 82:7796–7800.

Sigworth, F. J. 1983. Electronic design of the patch clamp. *In* Single Channel Recording. B. Sakmann and E. Neher, editors. Plenum Press, New York. 3–35.

Simmons, M. A., and H. C. Hartzell. 1985. Potassium currents in frog cardiac myocytes. Effects of acetylcholine, barium and potassium. *Society for Neuroscience Abstracts.* 11:227.1.

Trube, G. 1983. Enzymatic dispersion of heart and other tissues. *In* Single Channel Recording. B. Sakmann and E. Neher, editors. Plenum Press, New York. 69–76.

Downloaded from jgp.rupress.org on May 1, 2016